Anion Selective Recognition and Sensing by Novel Macrocyclic Transition Metal Receptor Systems. ^{1}H NMR, Electrochemical, and Photophysical Investigations

Paul D. Beer,*,† Fridrich Szemes,† Vincenzo Balzani,‡ Claudio M. Salà,‡ Michael G. B. Drew,§ Simon W. Dent,† and Mauro Maestri*,‡

Contribution from the Inorganic Chemistry Laboratory, University of Oxford, South Parks Road, Oxford OX1 3QR, U.K., Dipartimento di Chimica "G. Ciamician", Universita di Bologna, via Selmi 2, I-40126 Bologna, Italy, and Department of Chemistry, University of Reading, Whiteknights, Reading RG6 2AD, U.K.

Received July 24, 1997[⊗]

Abstract: A series of novel redox-active and photoactive ruthenium(II) and osmium(II) bipyridyl-, ferrocene-, and cobaltocenium-containing macrocyclic receptors with the dual capability of selectively sensing anionic guest species *via* electrochemical and optical methodologies have been prepared. Single-crystal X-ray structures of **7**·Cl^-, **7**·$2Br^-$, and **13**·$2OAc^-$ highlight the importance of hydrogen bonding and respective macrocyclic cavity size to the anion recognition process in the solid state. Proton NMR titration studies in deuterated DMSO solutions reveal these receptors form strong and remarkably selective complexes with Cl^-, $H_2PO_4^-$, and OAc^- anions dependent upon the flexibility, topology, and size of the receptor cavity. Cyclic and square-wave voltammetric investigations have demonstrated these receptors to electrochemically recognize Cl^-, $H_2PO_4^-$, and OAc^- anions. Photophysical studies reveal emission spectral recognition of Cl^- in acetonitrile solutions is displayed by **7**−**12**. With the hetero-dinuclear receptors **8**, **9**, and **12**, the rate constants of the energy transfer process responsible for the quenching of the luminescent ruthenium excited state significantly decreased in the presence of chloride anion.

Introduction

The molecular recognition of anionic guest species of biochemical and environmental importance by positively charged or neutral electron-deficient abiotic receptor molecules is an area of ever increasing research activity.[1,2] Anions play numerous fundamental roles in biological and chemical processes[3] as exemplified by the majority of enzymes binding anions as either substrates or cofactors, and many anions act as ubiquitous nucleophiles, bases, redox agents, and phase-transfer catalysts. Also their effects as environmental pollutants[4] have only recently been realized. Intensive arable farming has led to excess amounts of nitrate and phosphate contributing to the eutrophication of lakes and rivers. In addition the discharge of radioactive pertechnetate from the nuclear fuel cycle[5] and from radiopharmaceutical usage is of particular environmental concern. It is somewhat surprising then that the construction of specific ligands that have the capability of *sensing* anions *via* optical[6,7] and/or electrochemical[7] methodologies in polar organic and aqueous media has not been fully exploited. Czarnik,[6a,8] de Silva,[9] and Fabbrizzi[10] have recently described rare examples of anion fluorescent responsive types by combining the anthracene fluorophore with, respectively, polyammonium, guanidinium, and zinc(II) amine anion recognition sites. As part of a research program aimed at the design of innovative spectral and electrochemical sensory reagents for anions,[7] we are currently investigating systems based on transition metal organometallic and coordination receptor systems. In an effort to elucidate new anion selectivity trends, impart greater thermodynamic stability and sensitivity of sensing, we report here the syntheses of a series of novel ruthenium(II) and osmium(II) bipyridyl-, ferrocene-, and cobaltocenium-containing macrocyclic receptors. We have chosen such components because they are well-behaved redox-active species and also because of the well known luminescence properties of Ru(II) and Os(II) complexes of bipyridine-type ligands.[11] Extensive anion coordination investigations using X-ray crystallography, NMR spectroscopy, electrochemistry, and photophysical studies reveal

† University of Oxford.
‡ Universita di Bologna.
§ University of Reading.
⊗ Abstract published in *Advance ACS Abstracts,* November 15, 1997.

(1) Schmidtchen, F. P. *Nachr. Chem. Tech. Lab*. **1988**, *36*, 8. Katz, H. E. In *Inclusion Compounds*; Atwood, J. L., Davies, J. E. D., MacNicol, D. D., Eds.; Oxford University Press: New York, 1991; Vol. 4, p 391. Dietrich, B. *Pure Appl. Chem*. **1993**, *65*, 1457. Atwood, J. L.; Holman, J. T.; Steed, J. W. *Chem. Commun*. **1996**, 1401. Beer, P. D.; Smith, D. K. *Prog. Inorg. Chem*. **1997**, *46*, 1.

(2) Hawthorne, M. F.; Yang, X.; Knubler, C. *Angew. Chem., Int. Ed Engl.* **1991**, *30*, 1507. Sessler, J. L.; Burrell, A. K. *Top. Curr. Chem*. **1992**, *161*, 177. Bencini, A.; Bianchi, P.; Dapporto, E.; Garcia-Espana, M.; Micheloni, P.; Ramirez, J. A.; Pavletti, P.; Paoli, P. *Inorg. Chem*. **1992**, *31*, 1902. Reinhoudt, D. N.; Rudkevich, D. M.; Stauthamer, W. R. P. V.; Verboom, W.; Engersen, J. F. J.; Harkenna, S. J. *J. Am. Chem. Soc*. **1994**, *116*, 4341. Holman, K. T.; Halihan, M. M.; Steed, J. W.; Jurisson, S. S.; Atwood, J. L. *J. Am. Chem. Soc*. **1995**, *117*, 7848; Xu, X.; Vittal, J. J.; Puddephatt, R. J. *J. Am. Chem. Soc*. **1995**, *117*, 8362. Gale, P. A.; Sessler, J. L.; Kral, V.; Lynch, V. *J. Am. Chem. Soc*. **1996**, *118*, 5140. Kavallieratos, K.; de Gala, S. R.; Austin, D. J.; Crabtree, R. H. *J. Am. Chem. Soc*. **1997**, *119*, 2325.

(3) Frausto da Silva, J. J. R.; Williams, R. J. P. *Struct. Bonding (Berlin)* **1976**, *29*, 67.

(4) Mason, C. F. *Biology of Freshwater Pollution*, 2nd ed.; Longman: Harlow, 1991.

(5) Holm, E. *Radiochim. Acta* **1993**, *63*, 57.

(6) (a) Czarnik, A. W. *Acc. Chem. Res*. **1994**, *27*, 302. (b) Slone, R. V.; Yeon, D. I.; Calhoun, R. M.; Hupp, J. T. *J. Am. Chem. Soc.* **1995**, *117*, 11813.

(7) Beer, P. D. *Chem. Commun*. **1996**, 689.

(8) Vance, D. H.; Czarnik, A. W. *J. Am. Chem. Soc*. **1994**, *116*, 9397.

(9) de Silva, A. P.; Gunaratine, H. Q. N.; McVergh, C.; Maguire, G. E. M.; Maxwell, P. R. S.; O'Hanlon, E. *Chem. Commun*. **1996**, 2191.

(10) Fabbrizzi,L.; Francese, G.; Licchelli, M.; Perotti, A.; Taglietti, A. *Chem. Commun*. **1997**, 581.

(11) Sauvage, J.-P.; Collin, J.-P.; Chambron, J.-C.; Guillerez, S.; Coudret, C.; Balzani, V.; Barigelletti, F.; DeCola, L.; Flamigni, L. *Chem. Rev*. **1994**, *94*, 993.

S0002-7863(97)02509-2 CCC: $14.00

Scheme 1

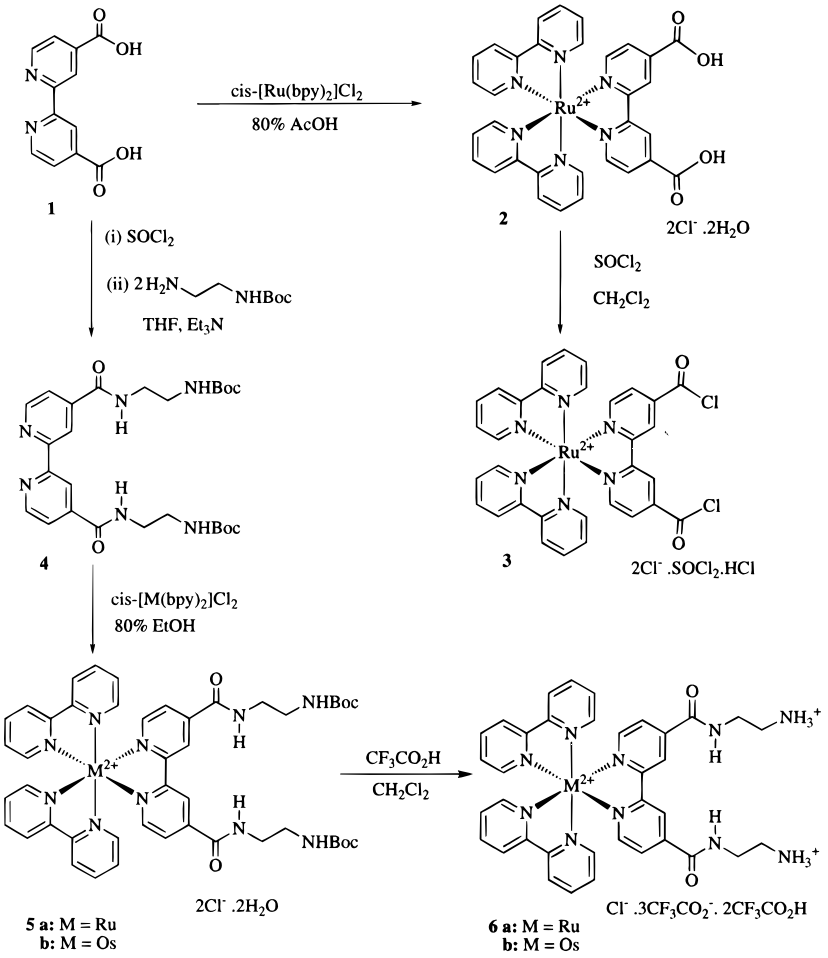

the topological nature and relative size of the macrocyclic cavity dictates the remarkable chloride, dihydrogen phosphate, or acetate anion selectivity trends these receptors display.[12]

Results and Discussion

Synthesis of Macrocyclic Anion Receptors. Taking into account the crucial importance of hydrogen bonding to the anion recognition process for our metallocene organometallic and acyclic and calix[4]arene heteroleptic ruthenium(II) tris-(bipyridyl) receptors,[7,13] the design of the target macrocyclic receptors featured amide (CONH) groups linking transition metal bipyridyl and metallocene subunits into various cyclic arrangements.

The preparation of the initial target synthons **3** and **6** for macrocyclization is shown in Scheme 1. 4,4′-Dicarboxy-2,2′-bipyridine (**1**)[14] was reacted with *cis*-$[Ru(bpy)_2Cl_2]\cdot 2H_2O$ in 80% acetic acid to afford the ruthenium(II) complex **2** in 94% yield. Treatment of **2** with excess thionyl chloride in dichloromethane gave **3** in quantitative yield. The reaction of **1** with thionyl chloride gave 4,4′-bis(chlorocarbonyl)-2,2′-bipyridine[15] which on condensation with 2 equiv of mono-Boc-protected ethylenediamine[16] produced **4** in 91% yield. Reaction of **4** with *cis*-$[M(bpy)_2Cl_2]\cdot 2H_2O$ (M = Ru, Os) gave the metal complexes **5a** and **5b** which on treatment with trifluoroacetic acid afforded the deprotected synthons **6a** and **6b**, isolated as mixed chloride−trifluoroacetate salts (Scheme 1).

Two synthetic procedures were employed for the preparation of the various macrocyclic tetraamides. The first procedure utilized the synthons **6a**,**b** in condensation reactions with the appropriate bis(acid chloride) under high dilution conditions in acetonitrile, to give after conversion to hexafluorophosphate salts the macrocyclic products **7**−**12** in 13−40% yields (Scheme 2). A single-step high-dilution procedure of condensing **3** and alkyl-, aryl-, and alkynyldiamines was used for the preparation of the symmetrical homo-dinuclear transition metal macrocyclic receptors **13**−**16** which were isolated as hexafluorophosphate salts in 18−46% yields (Scheme 3). It is noteworthy that receptor **11** was prepared in highest yield via the first macrocyclization synthetic route.

Solid State Structures of Anion Complexes. Slow evaporation of acetonitrile solutions of **7** in the presence of chloride and bromide anions and **13** with acetate gave anion complex crystals **7**·Cl^-, **7**·$2Br^-$, and **13**·$2AcO^-$ suitable for X-ray structural determinations.

All three structures show the ruthenium atom to be six-coordinate with a closely octahedral geometry. It is bonded to two unsubstituted bipyridine ligands as well as one further bipyridine ligand substituted to form a macrocyclic ring. In the chloride and bromide complexes of **7** this is a 21-membered ring with four amide groups which can be directed inward to form hydrogen bonds to an anionic guest. The two crystal structures show bromide and chloride respectively encapsulated within the macrocycle.

(12) Part of this work has been published as a preliminary communication: Beer, P. D.; Szemes, F. *J. Chem. Soc., Chem. Commun*. **1995**, 2245.

(13) Szemes, F.; Hesek, D.; Chen, Z.; Dent, S. W.; Drew, M. G. B.; Goulden, A. J.; Graydon, A. R.; Grieve, A.; Mortimer, R. J.; Wear, T.; Weightman, J. S.; Beer, P. D. *Inorg. Chem.* **1996**, *35*, 5868.

(14) Garelli, N.; Vierling, P. *J. Org. Chem.* **1992**, *57*, 3042.

(15) Whittle, C. P. *J. Heterocycl. Chem.* **1977**, *14*, 191.

(16) Kropcho, A. P.; Knell, C. S. *Synth. Commun.* **1990**, *20*, 2559.

Scheme 2

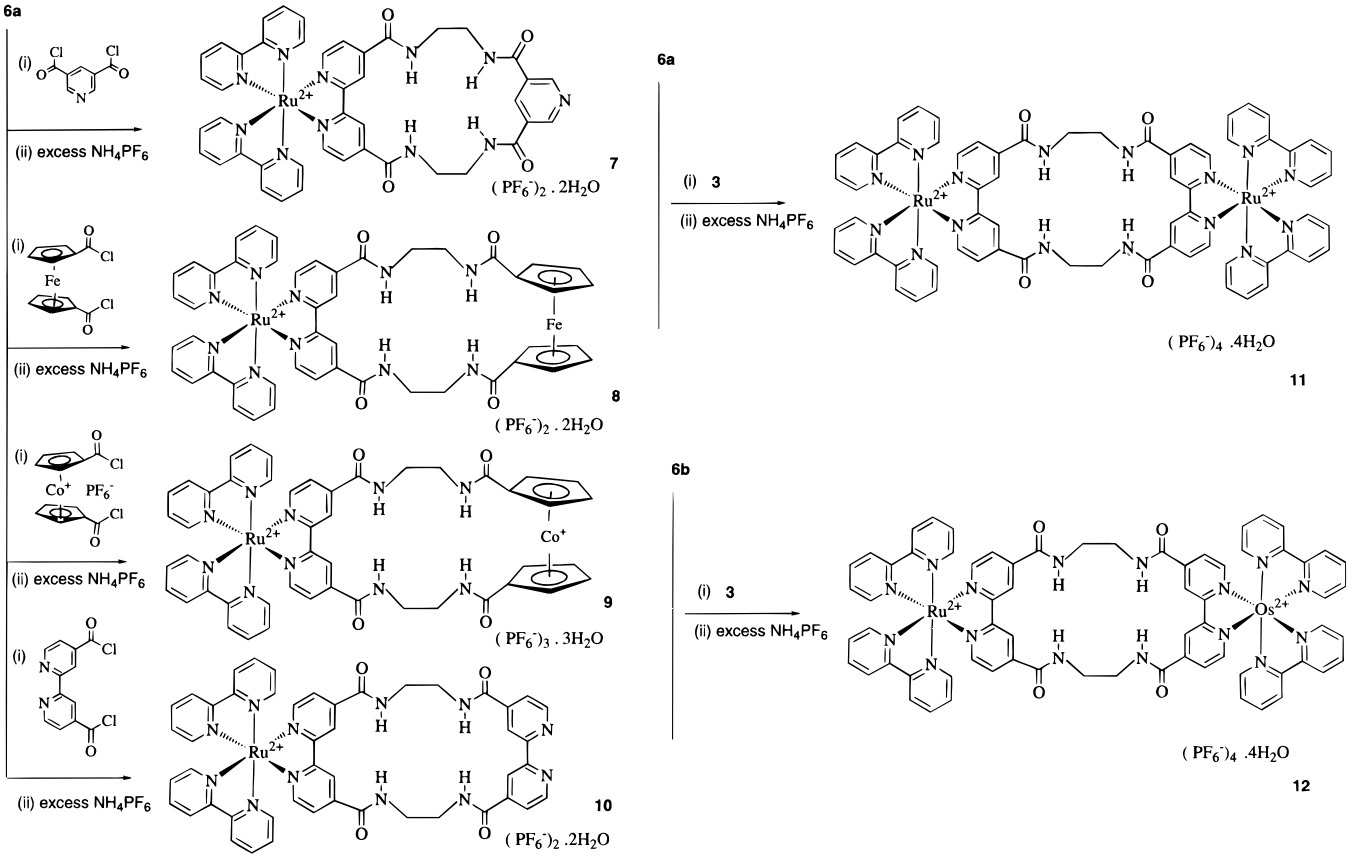

Scheme 3

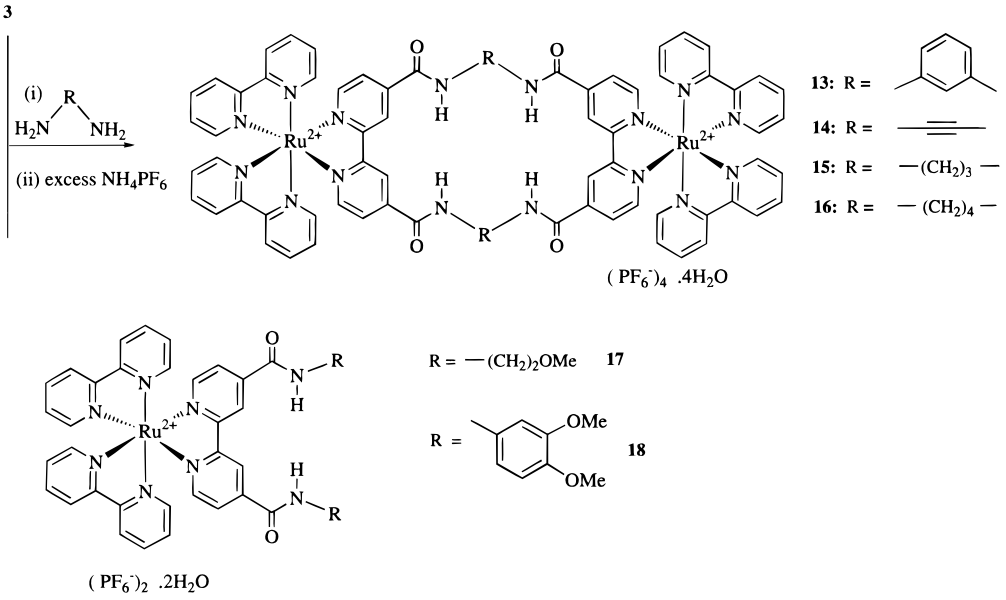

The structure of the bromide complex of **7** is shown in Figure 1 together with the atomic numbering scheme. The Ru−N bonds range from 2.083(8) to 2.124(9) Å. There are two bromide anions associated with the macrocycle. Br(1) is within the macrocycle cavity but hydrogen bonded to only three of the four amide groups in the macrocycle, *viz.*, N(102), N(205), and N(105) at 3.370, 3.434, and 3.657 Å, respectively. It is definitely not so bonded to N(202) as the Br···N distance is 4.238 Å. Apart from the four amide groups there is also the potential in the macrocycle to form C−H···Br hydrogen bonds.

Distances to carbon atoms clearly indicate some interaction as some are only slightly longer than the N···Br distances listed above. The shortest contact is to C(72) of 3.718 Å, but the distances to C(15) and C(18) are only slightly greater at 3.886 and 3.972 Å. The second bromide is disordered over two sites, 0.66 Å apart from both sites, and Br(2) and Br(3) are hydrogen bonded to N(202) at 3.446 and 3.369 Å and form longer contacts to C(18), 3.804 and 3.760 Å. The position of this bromide is well outside the plane of the macrocycle but enclosed within the pocket created by the fold in the macrocycle. Clearly the disorder is concomitant with this bromide being weakly bound within the macrocycle pocket.

The structure of the chloride complex of **7** is shown in Figure 2 together with the atomic numbering scheme. The Ru−N bond

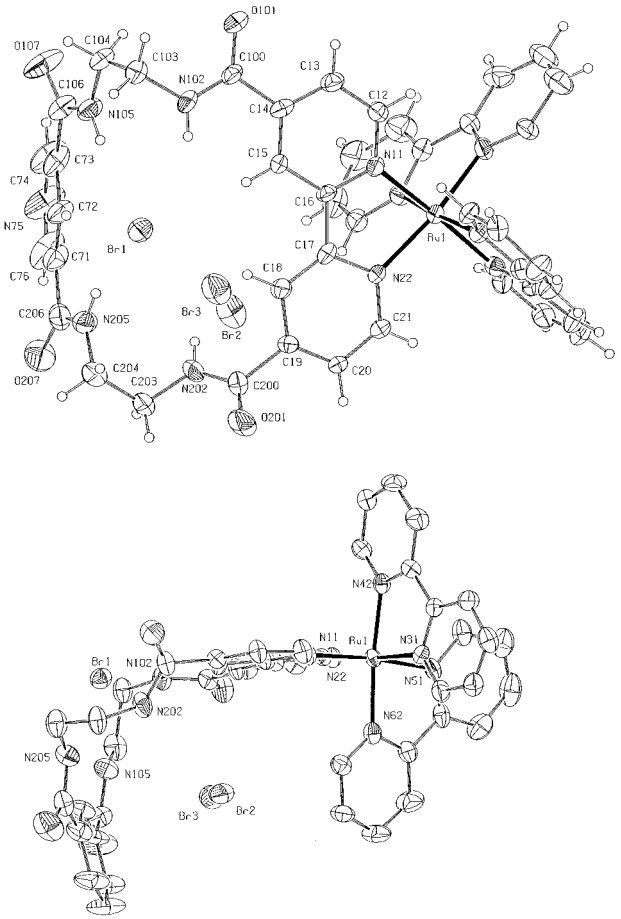

Figure 1. (a, top) The structure of **7**·2Br$^-$ with ellipsoids at 30% probability. The hydrogen atoms are shown as small circles with arbitrary radii. (b, bottom) The structure of **7**·2Br$^-$ with ellipsoids at 30% probability showing the overall shape of the macrocycle. Hydrogen atoms are omitted for clarity.

lengths range from 2.063(6) to 2.113(6) Å. Here only one chloride anion is associated with the macrocycle. The other chloride anion is disordered over several sites. Cl(1) is similar in position to Br(1) in that it forms hydrogen bonds to N(102), N(105), and N(205) with distances of 3.314, 3.395, and 3.540 Å but not to N(202) at 4.305 Å. This result allied to that obtained for the bromide complex indicates that it is not possible for all four amide nitrogen atoms to form hydrogen bonds to a monatomic anion.

The chloride anion also forms hydrogen bonds to C−H moieties. The distances to C(72), C(15), and C(18) are 3.550, 3.676, and 3.862 Å, respectively. The second chloride anion was disordered over several sites, but neither the site with the highest population (40%) nor any of the others form hydrogen bonds to any of the N−H groups of the macrocycle. Possibly as a consequence of this lack of hydrogen bonds, the macrocycle does not fold as much in the chloride complex as in the bromide analogue as is clearly shown in Figures 1b and 2b.

By contrast with the halide complexes of **7** the structure of **13**·2AcO$^-$ shows two metal octahedra linked through substituted bipyridyl moieties to form a 26-membered macrocycle. This is shown in Figure 3 together with the atomic numbering scheme. The complex cation contains a crystallographic center of symmetry. The Ru−N bond lengths range from 2.035(10) to 2.087(9) Å. As in the halide complexes of **7** each ruthenium atom is bonded to two unsubstituted and one substituted bipyridyl in an octahedral environment. Unlike the halide complexes, this macrocycle as is apparent from Figure 3b is

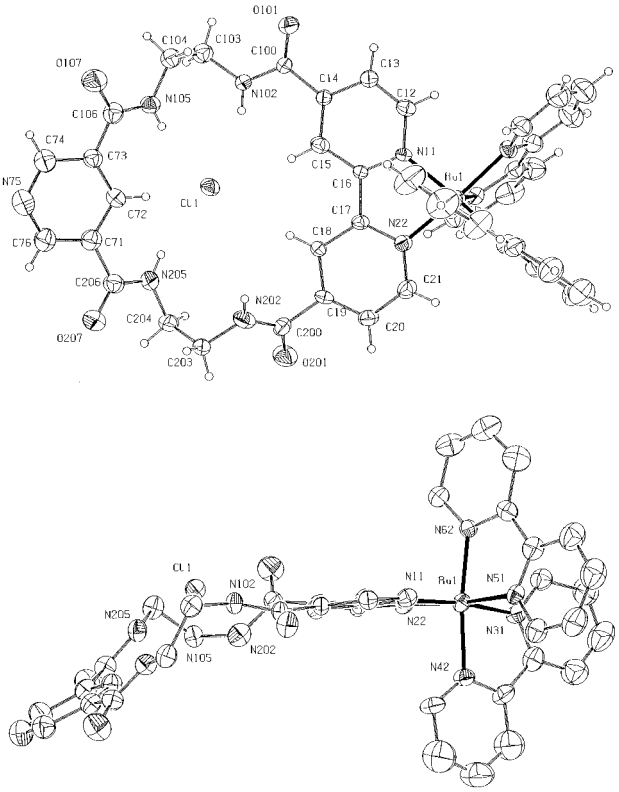

Figure 2. (a, top) The structure of **7**·Cl$^-$ with ellipsoids at 30% probability. The hydrogen atoms are shown as small circles with arbitrary radii. (b, bottom) The structure of **7**·Cl$^-$ with ellipsoids at 30% probability showing the overall shape of the macrocycle. Hydrogen atoms are omitted for clarity.

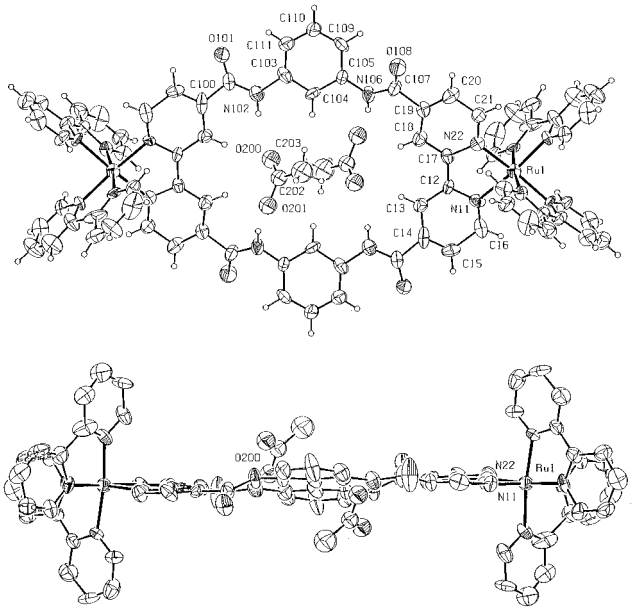

Figure 3. (a, top) The structure of **13**·2OAc$^-$ with ellipsoids at 30% probability. The hydrogen atoms are shown as small circles with arbitrary radii. There is a crystallographic center of symmetry. (b, bottom) The structure of **13**·2OAc$^-$ with ellipsoids at 30% probability showing the overall planar shape of the macrocycle. Hydrogen atoms are omitted for clarity.

closely planar. Two acetates are associated with the macrocycle, and each form two strong hydrogen bonds to two amide oxygen atoms. N(106)···O(201) is 2.781 Å and N(102)···O(200) is 2.894 Å. As can be seen from Figure 3 both oxygen atoms from the acetate can enter into the macrocycle cavity without requiring any significant fold.

Table 1. Stability Constants $K_a(M^{-1})^a$ of Receptors with Anions in DMSO-d_6

	anion		
receptor	Cl^-	AcO^-	$H_2PO_4^-$
7	5.0×10^3	1.4×10^4	1.2×10^2
8	9.9×10^3		
9	1.8×10^4	5.0×10^2	7.2×10^2
10	1.3×10^4	2.1×10^3	
11	4.0×10^4	3.6×10^3	no perturb.
12	4.9×10^4	1.3×10^2	0.4×10^2
13	3.0×10^3	$2.2 \times 10^{6\,b}$	$> 10^5$
14	3.0×10^2	6.9×10^2	$> 10^5$
15	0.6×10^2	3.7×10^2	$> 10^5$
16	3.7×10^2	7.3×10^2	$> 10^5$
17	1.5×10^2	3.5×10^2	1.3×10^3

[a] Errors ≤10%. [b] 2:1 anion:receptor complex, $(M^{-1})^2$.

Apart from the N−H···O hydrogen bonds, there are close contacts between C−H moieties and the anions, *viz*., C(13)···O(200) = 3.022 Å, C(104)···O(200) = 3.371 Å, C(18)···O(201) = 3.308 Å, and C(104)···O(201) = 3.408 Å, which are indicative of weak hydrogen bonds. Thus, each oxygen atom forms three hydrogen bonds, one to an amide N−H and two to aromatic C−H moieties.

Solution Anion Coordination Investigations. (a) ^{1}H NMR Titrations. The recognition of anions in solution was initially studied by ^{1}H NMR spectroscopy. The addition of tetrabutylammonium chloride or acetate to DMSO-d_6 ^{1}H NMR solutions of **7**−**16** resulted in substantial perturbations of most notably the respective amide, 3,3′-bipyridyl, 4-pyridyl, and cyclopentadienyl receptor protons. The resulting titration curves all suggested a 1:1 receptor:anion stoichiometry, with the exception of **13** which implied 1:2 receptor:anion stoichiometry. Analogous ^{1}H NMR titration experiments with dihydrogen phosphate gave contrasting results. Although large magnitudes of shifts were observed with receptors **7** and **13**−**16**, only very small perturbations of the respective macrocyclic protons of **8**−**10** and **12** were noted. In particular *no* ^{1}H or ^{31}P NMR evidence of $H_2PO_4^-$ binding was seen at all with **11** whereas with **13**, on the NMR time scale, a kinetically inert and thermodynamically very stable complex of **13**·2H_2PO_4 stoichiometry is formed.

The computer program EQNMR[17] was used to determine the stability constants from the ^{1}H NMR titration data, and the results are summarized in Table 1 which includes for comparison purposes stability constant data for acyclic receptor **17**. Clearly the size and topological nature of a receptor's macrocyclic cavity has a dramatic effect on the selectivity preferences a particular receptor exhibits. Compared to acyclic receptor **17**, the macrocyclic receptors **8**−**12** form much stronger chloride anion complexes by up to *ca*. 2 orders of magnitude and display the remarkable and rare Cl^- over $H_2PO_4^-$ selectivity preference. This is especially highlighted with **11** where no binding of $H_2PO_4^-$ is observed in DMSO which dramatically compares with a Cl^- stability constant of 40 000 M^{-1}. Interestingly the reverse selectivity trend $H_2PO_4^- > Cl^-$ is displayed by acyclic **17** and macrocycles **13**−**16**. In particular, the latter macrocyclic receptors form extremely stable complexes with $H_2PO_4^-$ (Table 1). The comparative size, flexibility, and degree of preorganization of the receptor cavity may account for these contrasting anion selectivity patterns which are discussed further using molecular modeling investigations in the next section.

The magnitudes of stability constants for acetate binding also vary dramatically (Table 1). The smallest macrocyclic receptor **7** forms a very strong complex with acetate and displays the $AcO^- > Cl^- > H_2PO_4^-$ selectivity trend whereas **10**−**12** exhibit the $Cl^- > AcO^- > H_2PO_4^-$ selectivity sequence. The larger macrocyclic receptors **14**−**16** along with acyclic **17** display $H_2PO_4^- > AcO^- > Cl^-$ selectivity, with **13** forming a very stable 2AcO^-: **13** stoichiometric solution complex in agreement with solid state X-ray crystallographic analysis discussed in the previous section.

Finally it is noteworthy that a comparison of the stability constant values of **10**−**12** reveals the additional coordinated ruthenium(II) metal cation present in **11** increases the thermodynamic stability of the Cl^- and AcO^- complexes of **10** and that with **12** osmium(II) is a more efficient Lewis acid center for binding Cl^-. This latter observation has also been noted in related acyclic dinuclear bipyridyl amide receptor systems.[18]

Molecular Modeling Investigations. Molecular modeling calculations were undertaken in an attempt to further rationalise the novel anion selectivity trends.

The crystal structure of the acyclic receptor **18**·chloride complex showed the halide anion formed six hydrogen bonds in an approximate hexagonal planar arrangement, two with amide nitrogen atoms at 3.34 and 3.37Å and four with phenyl hydrogens at 3.47, 3.48, 3.53, and 3.54 Å.[13] We took mean values of these distances (3.355, 3.495 Å) for subsequent calculations. The universal force field in CERIUS2[19] was utilized. Charges were set using the Q_{eq} method. The ethane spacer in **11** allows the eight hydrogen atoms to be directed into the cavity (four from 2,2′-bipyridyl rings, four from amide nitrogen atoms) to form hydrogen bonds to one chloride anion. Cl···H distances were constrained to the above mean values and minimization on **11**·Cl^- showed an energy of interaction of −196 kcal mol^{-1} (defined as energy of the host/guest complex − energy of the host − energy of the guest). The cavity is significantly distorted from planarity to allow for these eight bonds.

With phenyl spacers as in **13**, there are ten hydrogen atoms directed toward the cavity, but one chloride anion can only form six hydrogen bonds at one end to four phenyl hydrogen and two amide nitrogen atoms in a plane. The arrangement is very similar to that found in the acyclic **18**·chloride complex, and the energy of interaction is calculated as −152 kcal mol^{-1}. It is of course possible for two chloride anions to occupy either end of the cavity, each being bonded uniquely to four hydrogen atoms and sharing two hydrogen atoms from the phenyl spacers, but the additional interaction energy for this second chloride anion is only −21 kcal mol^{-1}. In this model, the two chloride anions are 3.42 Å apart. With the aliphatic spacers in **15** and **16** there are only four hydrogen atoms available for each chloride, and this may account for the lower stability constants.

The arrangement of hydrogen bonds in **8** and **9** will be different from that in **7**. The two cyclopentadiene rings will be only ca. 4.1 Å apart and this will ensure that the two amide groups are similarly distanced compared to the 5.25 Å in **7**. This ensures that the chloride anion cannot enter the cavity in a planar fashion, but all four amide hydrogens can be directed to one side of the plane and hydrogen bonded to one chloride anion with an energy of interaction of −135 kcal mol^{-1}.

With the bipyridyl link in **10**, the N···N distance increases to ca 7.5 Å, too far for a chloride to hydrogen bond to both nitrogen atoms without significant increase in strain. Even so an interaction energy of −161.0 kcal mol^{-1} is obtained. When the interaction is confined to just three of the nitrogen atoms, an energy of −204 kcal mol^{-1} is found, and this arrangement seems likely to be the structure of the **10**·Cl^- complex.

(17) Hynes, M. J. *J. Chem. Soc., Dalton Trans.* **1993**, 311.

(18) Beer, P. D.; Dent, S. W.; Hobbs, G. S.; Wear, T. J. *Chem. Commun.* **1997**, 99.

(19) Cerius 2 Molecular Simulations Inc., Cambridge, U.K., and San Diego, CA.

In the crystal structure of the complex **13**·2AcO$^-$ with a phenyl space, the N···N distance is 6.72 Å concomitant with a N−H···O−C−O···H−N moiety.

In **7**, **8**, and **9** this distance is maintained between the amide groups adjacent to the Ru(bpy)$_3$ moiety, but the distance between the other amide groups is reduced to *ca*. 5.25 Å (**7**) or *ca*. 4.1 Å (**8**, **9**) which precludes the binding of two anions in the complex.

In **10** the distance between these nitrogen atoms is 7.5 Å, and hydrogen bonds can be formed to an additional acetate, but all the low-energy conformations of the complex are folded so that there is insufficient room for two acetates. It is interesting that, in the lowest energy conformations of **11** and **12**, intramolecular hydrogen bonds were formed between adjacent amide C═O···H−N moieties. It seems likely that these could also be present in **14**, **15**, and **16**.

The interaction of phosphate with these macrocycles is more difficult to model because there are many different ways in which the phosphate can interact with the macrocycle. In the crystal structure of **18**·H_2PO_4,[13] the phosphate formed three hydrogen bonds to the receptor. Of course the phosphate oxygen atom can be acting as either donor or acceptor for any of these bonds. In structures **13**−**16** inclusive, while the phosphate could efficiently interact with three atoms of the macrocycle, it is more favorable to react with just two (e.g., for **13** the energy of interaction with two bonds is −104.2 kcal mol^{-1} compared to −87.8 for three bonds); indeed this is possible whether the C═O group or the N−H group is directed at the phosphate. In all these compounds the two phosphates can form hydrogen bonds in the manner of the acetates in **13**. Unlike the acetates, however, the phosphates can interact with a carbonyl oxygen instead of an N−H, and this may account for the much higher stability constants for phosphate.

Clearly the lower stability constants in the smaller macrocycles are in part due to the fact that two phosphates cannot be hydrogen bonded, because the distance between the N−H groups away from the Ru(bpy)$_3$ moiety is significantly less than is necessary for a N−H···O−P−O···H−N linkage. In addition the fold in **7** ensures that the two N−H groups closest to the Ru(bpy)$_3$ moiety are directed away from each other, and this reduces the possibility of a bridging hydrogen bonded phosphate.

The very low value in **12** and the zero value in **11** are hard to explain because it is clearly possible for the phosphate to form hydrogen bonds to the macrocycle. One possibility is that intramolecular hydrogen bonds are formed which preclude the phosphate from binding.

(b) Electrochemical Anion Recognition Studies. Cyclic and square-wave voltammetry was used to investigate the electrochemical anion recognition properties of the receptors **7**−**12** in acetonitrile, and the results are summarized in Table 2.

On account of the electron-withdrawing nature of the carbonyl amide moieties, the least cathodic bipyridyl ligand-centered reduction couple can be assigned to the amide-substituted bipyridyl group present in each receptor. Interestingly it is this redox couple of the ruthenium(II) bipyridyl redox system that exclusively undergoes significant cathodic perturbations on addition of anionic guest species (Table 3). This observation, in agreement with solid state complex structures and ^{1}H NMR titration studies, suggests that anion binding takes place in the amide−bipyridyl vicinity of the respective receptor. With **8** and **9** anion induced cathodic perturbations of the respective metallocene redox couples of up to 110 mV with chloride anion were also noted (Table 3).

Photophysical Investigations. The photophysical investigations have been carried out on the mononuclear complexes **7** and **10**, the homodinuclear Ru complex **11**, and the heterodinuclear Ru−Fe (**8**), Ru−Co (**9**), and Ru−Os (**12**) complexes. The experiments have been performed in acetonitrile solution at room temperature and in a butyronitrile rigid matrix at 77 K. The most important data are gathered in Table 4, where the data for the parent Ru(bpy)$_3^{2+}$ compound are also reported for comparison purposes. Under the experimental conditions used (concentration on the order of 10^{-4} M), bimolecular quenching processes can be ruled out.

Table 2. Electrochemical Data[a]

receptor	metal-based $E_{1/2}$ (V)	Bpy-based +2/+1 $E_{1/2}$ (V)	Bpy-based +1/0 $E_{1/2}$ (V)	Bpy-based 0/−1 $E_{1/2}$ (V)
[Ru(bpy)$_3$][PF$_6$]$_2$	1.025	−1.610	−1.820	−2.115
7	1.100	−1.525	−1.715	−2.005
8	1.035 (Ru^{II}/Ru^{III}) 0.390 (Fe/Fe$^+$)	−1.495	−1.705	−2.110
9	1.000 (Ru^{II}/Ru^{III}) −0.915 (Co/Co$^+$)	−1.500	−1.730	−2.200
11	0.990	−1.470	−1.825	−2.075
12	0.985 (Ru^{II}/Ru^{III}) 0.560 (Os^{II}/Os^{III})	−1.430	−1.790	−2.080

[a] Obtained in acetonitrile solution containing 0.1 mol dm^{-3} [^{n}Bu$_4$N$^+$][PF$_6^-$] as supporting electrolyte. Solutions were 5×10^{-4} mol dm^{-3} in receptor, and potentials were determined with reference to a Ag/Ag$^+$ electrode (330 ± 5 mV vs SCE) at 21 ± 1 °C and 100 mV s^{-1} scan rate.

Table 3. Cathodic Shifts Induced upon First (Substituted) Bipyridyl Redox Wave on Addition of Anionic Guests

receptor	$\Delta E_{1/2}$ (mV)[a] (Cl^-)	$\Delta E_{1/2}$ (mV)[a] ($H_2PO_4^-$)	$\Delta E_{1/2}$ (mV)[a] (AcO^-)
7	30	20	55
8	40 60[b]	15	20
9	90 110[b]	ppt	10
11	110	< 5	15
12	125	ppt	20

[a] Cathodic shifts induced upon substituted bipyridyl redox waves on addition of excess anions in acetontrile solution. Solutions were 5×10^{-4} mol dm^{-3} in receptor and anions were added as 6.25 mM solutions (ppt = precipitation). [b] Shift in Fc/Fc$^+$ or Co/Co$^+$ redox couple.

Macrocycles 7 and 10. Macrocycles **7** and **10** are mononuclear heteroleptic Ru complexes containing two simple bpy ligands and a bpy ligand which carries electron-withdrawing carbonyl amide substituents. It is well known that the intense absorption band with I_{max} = 450 nm and the long-lived luminescence band (I_{max} = 611 nm and τ = 200 ns in aerated acetonitrile solution at room temperature) shown by Ru(bpy)$_3^{2+}$ are due to spin-allowed and, respectively, spin-forbidden metal-to-ligand charge-transfer transitions.[20] Because of their heteroleptic nature, **7** and **10** are expected to exhibit two types of MLCT transitions. More specifically, in view of the electron withdrawing nature of the carbonyl amide substituents, the Ru → macrocycle transitions must lie at slightly lower energy than the Ru → bpy ones. As a consequence, for **7** and **10** the absorption band at around 450 nm is broader than that of Ru(bpy)$_3^{2+}$, and the emission band (which is due to the lowest energy spin-forbidden excited state, involving the macrocyclic ligand) is red-shifted compared to that of Ru(bpy)$_3^{2+}$. The photophysical properties of the two compounds are almost identical, showing that the remote pyridine and bipyridine moieties have no effect on the metal and on its coordination

(20) Balzani, V.; Juris, A.; Venturi, M.; Campagna, S.; Serroni, S. *Chem. Rev.* **1996**, *96*, 759.

Table 4. Photophysical Data

	absorbance[a]		room temp emission[a]				77 K emission[b]		
compound	λ_{max}[c] (nm)	ϵ (M^{-1} cm^{-1})	λ_{max}[d] (nm)	τ[e] (ns)	$\Phi \times 10^2$ [f]	k_q[g] (s^{-1})	λ_{max}[c] (nm)	τ[e] (μs)	k_q[g] (s^{-1})
7	468	13600	655	330	1.5		615	5.7	
7·Cl^-			646	350					
8	468	13400	654	13 and 310	0.4	7×10^7	616	0.15	7×10^6
8·Cl^-			647	42 and 345	0.6	2×10^7			
9	470	14800	655	61 and 285	0.4	1×10^7	617	0.9	1×10^6
9·Cl^-			649	132 and 472	1.0	5×10^6			
10	470	13000	658	340	1.4		616	5.8	
10·Cl^-			650	360					
11	472	25500	658	340	2.0		620	6	
11·Cl^-			652	384	2.6				
12	450	22300	Ru 658	0.9	0.13	1×10^9	755	0.0047	2×10^8
			Os 783	46				0.87	
12·Cl^-			Ru	1.4		7×10^8			
			Os	46					
$Ru(bpy)_3^{2+}$	450	15000	615	200	1.6		580	5.8	

[a] Acetonitrile. [b] Butyronitrile. [c] Wavelength of the lowest energy absorption band. [d] Uncorrected wavelength of the emission maxima. [e] Luminescence emission lifetime (±10%). [f] Luminescence emission quantum yield values (±30%). [g] Intramolecular quenching constant.

environment. We have also examined other compounds like those of the **5a** and **6a** family, and we have found that they exhibit the same properties as **7** and **10**.

Macrocycle 11. This macrocycle is a dinuclear Ru complex where the two metal-based units are equivalent. Its photophysical properties are very similar to those of its parent mononuclear compound **10**.

Macrocycles 8 and 9. Macrocycles **8** and **9** are heterodinuclear complexes made of a potentially luminescent Ru−bpy type moiety with an appended ferrocene (Fc) and, respectively, cobaltocenium (Co^+) moiety. It has been reported[21] that in fluid solution at room temperature the luminescent excited state of $Ru(bpy)_3^{2+}$ is quenched with an almost diffusion controlled rate constant ($k_q = 5.9 \times 10^9$ M^{-1} s^{-1}) by ferrocene and with a somewhat lower rate constant ($k_q = 1.5 \times 10^8$ M^{-1} s^{-1}) by the cobaltocenium ion. The zero−zero excited state energy (E^{00}) of the Ru-based moiety of **8** and **9** (~2.0 eV, estimated from the emission maximum at 77 K) is certainly larger than the energy of the lowest excited state of ferrocene (estimated to be in the range between 1.8[22] and 1.1[23] eV) and cobaltocenium ion (not known, but presumably a little larger than that of ferrocene[21]). Therefore, quenching by energy transfer of the luminescent excited state of the Ru-based moiety by the appended metallocene unit is energetically allowed in both cases, but more so in compound **8**. Quenching by electron transfer is only marginally allowed from a thermodynamic viewpoint in both compounds, as one can estimate[24] from the zero−zero excited state energy of the Ru-based moiety and the E^0 values (eV) of the reduction potentials of the couples involved (Table 2):

$$\Delta G\ (\text{eV}) = -E^{00} - E^0(\text{Ru(bpy)}_3^{2+/1+}) + E^0(\text{Fc}^{+/0}) \approx -0.1\ \text{eV} \quad (1)$$

$$\Delta G\ (\text{eV}) = -E^{00} + \text{E}^0(\text{Ru(bpy)}_3^{3+/2+}) - E^0(\text{Co}^{+/0}) \approx -0.1\ \text{eV} \quad (2)$$

In a rigid matrix at 77 K, the electron transfer process would clearly be endoergonic because of the lack of repolarization of the solvent molecules.[25]

Comparison of the results obtained for the dinuclear compounds **8** and **9** with those of the parent mononuclear compounds **7** and **10** shows that emission occurs at approximately the same wavelength, confirming that the Ru-based unit is not strongly perturbed by the nature of the remote part of the macrocycle ligand. The emission quantum yield, however, is about 5 times lower for **8** and **9**, indicating the presence of a quenching process. It is also important to note that whereas **7** and **10** show the normal monoexponential decay for the luminescence intensity, the binuclear compounds **8** and **9** exhibit a biexponential decay. For the Ru−Fe complex **8**, we have found a short (13 ns) and a long (310 ns) decay, whose contributions to the emission intensity are 15 and 85%, respectively. For the Ru−Co complex **9**, the decay lifetimes are 61 and 285 ns, with contributions 65 and 35%, respectively. These results indicate that there are two distinct emitting species in each one of these systems.

An obvious possible explanation of the biexponential luminescence decay would be the presence, in the samples of **8** and **9**, of a Ru−bpy-based impurity, e.g., of some residual amount of a precursor of type **5a** or **6a**. As mentioned above, the photophysical properties of precursor-type compounds were therefore examined and found to coincide with those of the mononuclear compounds **7** and **10**. This shows once again that the photophysical properties of the Ru-based unit are not strongly perturbed by the groups appended (by a $-(CH_2)_2-$ spacer) to the amide substituents. The presence of mononuclear impurities can be discounted on the following basis: (i) for both compounds, and particularly for **9**, none of the two decay times coincides with that observed for the mononuclear complexes; (ii) on the assumption that the longer lifetime found for **8** is due to a mononuclear Ru-based compound like **6a**, **7**, or **10**, from the relative contributions of the long (85%) and short (15%) decays one should conclude that in the prepared sample of **8** the amount of impurity should be on the order of 25%. In fact, the sample was carefully purified by column chromatography, and it did not contain sizable amounts of other compounds.

We believe that a possible explanation for the observed biexponential decays in compounds **8** and **9** may be given on the basis of the presence of two conformers (or family of

(21) Wrighton, M. S.; Pdungsap, L.; Morse, D. L. *J. Phys. Chem.* **1975**, *79*, 66.
(22) (a) Farmilo, A.; Wilkinson, F. *Chem. Phys. Lett.* **1975**, *34*, 575. (b) Lee, E. J.; Wrighton, M. K. *J. Am. Chem. Soc.* **1991**, *113*, 8562.
(23) Balzani, V.; Bolletta, F.; Scandola, F. *J. Am. Chem. Soc.* **1982**, *102*, 2152.
(24) Balzani, V.; Bolletta, F.; Gandolfi, M. T.; Maestri, M. *Top. Curr. Chem.* **1978**, *75*, 1.
(25) (a) Gaines, G. L., III.; O'Neil, M. P.; Svec, W. A.; Niemczyk, M. P.; Wasielewski, M. R. *J. Am. Chem. Soc.* **1991**, *113*, 719. (b) Chen, P.; Meyer, T. J. *Inorg. Chem.* **1996**, *35*, 5520.

conformers) which, because of the relative rigidity of the amide moieties, do not interchange within the lifetime of the excited state and therefore do experience different intramolecular quenching rates.[26] In one conformer the appended metallocene moiety would be relatively close to the Ru-based moiety, and would therefore quench efficiently the luminescent excited state, whereas in the other conformer the two moieties would be somewhat more separated, with the consequence of a smaller quenching rate. Within this hypothesis, the rate constants for the quenching processes can be obtained by the equation

$$k_q = 1/\tau - 1/\tau^o \quad (3)$$

where τ^o is the excited state of the Ru-based moiety in the absence of quenching (taken to be 340 ns, as for the mononuclear compounds **7** and **10** and the dinuclear compound **11**), and τ is the observed lifetime. The values of the rate constants are shown in Table 4. As one can see, the quenching constants are higher for compound **8** than for compound **7**, thereby reproducing the trend observed for the bimolecular quenching of $Ru(bpy)_3^{2+}$ by ferrocene and cobaltocenium ion.[21] The small values of the rate constants, compared with the almost diffusion-controlled bimolecular quenching in the case of $Ru(bpy)_3^{2+}$ by ferrocene, can be taken as an indication of a rigid structure of the macrocycle which prevents a close approach of the two moieties. The relatively small increase of the rate constants in going from rigid matrix to fluid solution could be due to a contribution of electron transfer quenching under the former experimental condition, but it is perhaps more likely due to the increased flexibility of the system at higher temperature.

Macrocycles 11 and 12. The macrocyclic compounds **11** and **12** can be viewed as dinuclear complexes of a bridging ligand where two equivalent bpy type units are separated by a tetraamide spacer. A great number of such dinuclear compounds have recently been prepared, and their photophysical properties have been investigated.[11] The homodinuclear compound **11** exhibits photophysical properties almost identical to those of its monocuclear parent **10**, as it always happens when the spacer linking the two metal-based units is aliphatic in nature. The lack of a substantial electronic interaction between the two metal-based units is consistent with the electrochemical results which show that in the Ru−Os compound **12** oxidation of the Ru moiety occurs at practically the same potential as in the Ru−Ru compound **11**. In the Ru−Os compound **12**, both the metal-containing units are potentially luminescent ($Os(bpy)_3^{2+}$ is known to exhibit a relatively weak emission band at 743 nm, with $\Phi = 5 \times 10^{-3}$ and $\tau = 60$ ns in deaerated acetonitrile solution).[27] Accordingly with this expectation, two emission bands are actually seen at the expected wavelengths (658 nm for the Ru-based moiety and 783 for the Os-based one at room temperature). It should be noted, however, that both the quantum yield and the lifetime of the Ru-based emission are much smaller than in the dinuclear complex. This shows that the Os-based moiety has a quenching effect on the Ru-based one. Using eq 3, the value of the quenching constant is 1×10^9 s^{-1} at room temperature and 2.1×10^8 s^{-1} at 77 K (Table 4). Using the above discussed relationship and the electrochemical data of Table 2 for the pertinent couples, one can see that quenching by electron transfer is thermodynamically almost isoergonic:

$$\Delta G\ (\text{eV}) = -E^{00} - E^0(Ru(bpy)_3^{2+/1+}) + E^0(Os(bpy)_3^{3+/2+}) \approx 0\ \text{eV} \quad (4)$$

This means that electron transfer quenching cannot account for the very fast quenching rates. Energy transfer, on the contrary, is thermodynamically allowed since the lowest excited state of the Os-based moiety, estimated from the maximum of the emission band at 77 K, is about 1.64 eV. The occurrence of a fast quenching process even in rigid matrix at 77 K is consistent with an energy transfer mechanism. Definitive evidence for energy transfer from the Ru-based moieties of **12** is given by the excitation spectrum, which closely matches the absorption spectrum. This means that substantially all the light absorbed by the complex, regardless of whether it is absorbed in the Ru-based or Os-based moiety, leads to emission from the Os-based excited state with the same efficiency.

One can ask why energy transfer is very fast in compound **12** and very slow in compounds **8** and **9**. The reason for such different behavior lies most likely in the much stronger overlap between donor emission ($I_{max} = 670$ nm) and acceptor absorption. $Os(bpy)_3^{2+}$ shows a very broad, relatively intense ($\epsilon >$ 1000 M^{-1} cm^{-1}) absorption band up to 700 nm, whereas ferrocene and cobaltocenium ion have a very weak band (ϵ on the order of 100 M^{-1} cm^{-1}) with a maximum at $\lambda < 500$ nm.[21] The molar absorption coefficients of the acceptor band intervene explicitly in determining the overlap integral in the Förster energy transfer mechanism.[28]

Effect of Cl^- Anions. In agreement with previously reported results,[7,12] addition of chloride anions to acetonitrile solutions of complexes **7**−**12** resulted in a slight blue shift (5−10 nm) and a marked increase of emission intensity (e.g., +30% for **11** and **12** and 100% for **9**). A concomitant, moderate increase in the emission lifetimes was also observed (see Table 4). Results obtained from Cl^- titration of the emission intensity are consistent with the formation of chloride−complex adducts of 1:1 stoichiometry for all the complexes. As we have seen above, the luminescent excited state is that involving the macrocyclic ligand. As expected (and shown by the electrochemical results) anion coordination makes the bpy moiety of the macrocyclic ligand more difficult to reduce. This is the reason for the blue shift of the emission band. The intensity and lifetime enhancement of the luminescence emission can be explained by the formation of a receptor−anion complex that increases the rigidity of the receptor, thereby disfavoring the nonradiative decay processes.

For the hetero-dinuclear receptors **8**, **9**, and **12**, a chloride effect was also observed on the rate constant of the energy transfer process responsible for the quenching of the luminescent excited state of the ruthenium bipyridyl moiety. In all cases, the energy transfer rate constant decreases upon Cl^- coordination, indicating a decrease of the electronic interaction between the excited Ru-based unit and the appended quencher moiety.

Conclusions

The syntheses of a series of novel redox-active and photoactive ruthenium(II) and osmium(II) bipyridyl-, ferrocene-, and cobaltocenium-containing macrocyclic receptors that have the capability to selectively complex and sense anionic guest species *via* electrochemical and spectral methodologies have been achieved.

(26) For an example of conformers in trinuclear Ru−Os metal complexes attributed to the rigidity of the amide group, see: Belser, P.; von Zelewsky, A.; Frank, M.; Seel, C.; Vogtle, F.; DeCola, L.; Barigelletti, F.; Balzani, V. *J. Am. Chem. Soc.* **1993**, *115*, 4076.

(27) Kalyanasundaram, K. *Photochemistry of Polypyridine and Porphyrin Complexes;* Academic Press: London, U.K. 1992.

(28) See, e.g.: Baltrop, J. A.; Coyle, J. D. *Principles of Photochemistry*; John Wiley & Sons: Chichester, U.K., 1978.

The solid state structures of chloride and bromide anion complexes of **7** and an acetate complex of **13** have been determined by X-ray analysis and highlight the importance of hydrogen bonding and respective macrocyclic cavity size to the overall anion recognition process. Proton NMR titration investigations in deuterated DMSO solutions have shown these receptors not only form thermodynamically stable anion complexes but also exhibit remarkable anion selectivity trends. For example, **11** displays outstanding selectivity for Cl^- over $H_2PO_4^-$; a stability constant of 40 000 M^{-1} for Cl^- compares with no evidence of binding of $H_2PO_4^-$ at all in DMSO solutions. In contrast the relatively larger macrocyclic receptors **13**−**16** exhibit the reverse selectivity trend, and the smallest macrocyclic receptor **7** forms a very strong and selective complex with acetate in preference to Cl^- and $H_2PO_4^-$. Evidently with this new class of macrocyclic anion receptor these selectivity findings suggest the comparative size, degree of preorganization, and topological nature of the macrocyclic receptor cavity crucially influences the anion recognition selection process. Electrochemical investigations have demonstrated that these receptors electrochemically sense Cl^-, $H_2PO_4^-$, and OAc^- anions via significant cathodic perturbations of respective amide-substituted bipyridyl and metallocene redox couples. Photophysical studies reveal a marked increase of emission intensity and moderate increase of emission lifetimes result from the addition of chloride to acetonitrile solutions of **7**−**12**. Interestingly for the hetero-dinuclear receptors **8**, **9**, and **12** the presence of bound Cl^- caused the rate constants of the energy transfer process responsible for the quenching of the luminescent excited state of the ruthenium bipyridyl moiety to significantly decrease. Thus, having demonstrated that this new macrocyclic class of anion receptor can selectively bind and detect anions via electrochemical and optical techniques, their fabrication into electronically conducting polymeric supports and optical fibers could produce prototype sensory devices of commercial interest.

Experimental Section

Instrumentation. NMR spectra were recorded at 25 °C on a Varian Unity Plus 500 MHz spectrometer which functions at 500 MHz for ^{1}H and at 125.7 MHz for ^{13}C NMR. Chemical shifts (ppm) are relative to those of the deuterated solvents. ^{13}C and ^{1}H NMR spectra were completely assigned using two-dimensional correlated NMR experiments (COSY). Fast atom bombardment (FAB) and electrospray (ES) mass spectrometry were performed by the EPSRC Mass Spectrometry Service at University College, Swansea. A Perkin-Elmer Model 300 fluorescence spectrophotometer was used for recording the fluorescence emission spectra.

Elemental analyses were performed at the Inorganic Chemistry Laboratory, University of Oxford. Melting points are uncorrected.

Solvent and Reagent Pretreatment. Dry solvents were used wherever necessary: dichloromethane (CH_2Cl_2) and acetonitrile were distilled from CaH_2; tetrahydrofuran (THF) was distilled from benzophenone ketyl; triethylamine was dried over KOH; demineralized water was used at all times; deuterated solvents were kept over 4 Å activated molecular sieves. All reactions were carried out in a nitrogen atmosphere, and the solvents were purged with nitrogen prior to use. Unless stated, commercial grade chemicals were used without further purification. 2,2′-Bipyridine-4,4′-dicarboxylic acid,[14] 4,4′-bis(chlorocarbonyl)-2,2′-bipyridine,[15] *N*-(tert-butoxycarbonyl)-1,2-diaminoethane,[16] 3,5-bis(chlorocarbonyl)pyridine,[29] 1,1′-bis(chlorocarbonyl)ferrocene,[30] 1,1′-bis(chlorocarbonyl)cobaltocenium chloride,[31] and 1,4-diamino-2-butane[32] were synthesized according to literature procedures.

Chromatography. Column chomatography of the ruthenium complexes was performed on silica gel (type 60G, Fluka), pretreated with the eluent. Thin layer chromatography (TLC) was performed on silica gel 60F-254 (Merck), using a mixture of acetic acid, ethanol, and water (1:1:1) as the mobile phase.

^{1}H NMR Titrations. The inital concentration of the titrated receptor molecules in DMSO-d_6 was 3.64×10^{-3} mol/L. This was gradually diluted with a 0.1 mol/L solution of tetrabutylammonium salts of anions.

Syntheses. In the following NMR spectroscopic data Pyr indicates the substituted and Bp the unsubstitued 2,2′-bipyridine nuclei, ov indicates the overlapping proton NMR peaks, and Dinic indicates the peaks of 3,5-substituted pyridine nuclei.

(4,4′-Dicarboxy-2,2′-bipyridine)bis(2,2′-bipyridine)ruthenium-(II) Dichloride Dihydrate (2). A mixture of 2,2′-bipyridine-4,4′-dicarboxylic acid (2.44 g, 10 mmol) and *cis*-bis(2,2′-bipyridine)-ruthenium(II) dichloride dihydrate (5.2 g,10 mmol) in 80% acetic acid (100 mL) was stirred for 5 h under reflux, and the solvent was removed in vacuo. The resulting dark red solid was dissolved in a minimum amount of ethanol (50 mL) in the presence of concentrated hydrochloric acid (0.5 mL), the solution was filtered though Celite, the filtrate was concentrated to 40 mL, and the diacid was precipitated by gradual addition of diethyl ether (∼100 mL). After stirring for 1 h at room temperature, the dark red product **2** was separated, washed with diethyl ether and dried at 60 °C: yield 7.2 g (94%); ^{1}H NMR (DMSO-d_6) δ 9.24 (s, 2H, Pyr 3,3′), 8.86 (m, 4H, Bp 3,3′), 8.18 (m, 4H, Bp 4,4′), 7.91(d, J = 5.8 Hz, 2H, Pyr 6,6′), 7.86 (dd, J = 5.8 and 1.1 Hz, 2H, Pyr 5,5′), 7.76−7.71 (m, 4H, Bp 6,6′), 7.57−7.48 (m, 4H, Bp 5,5′). Anal. Calcd for $C_{32}H_{28}N_6O_6Cl_2Ru$: C, 50.27; H, 3.69; N, 10.99; Ru, 13.22. Found: C, 50.27; H, 3.88; N, 10.61; Ru, 13.52.

[4,4′-Bis(chlorocarbonyl)-2,2′-bipyridine]bis(2,2′-bipyridine)ruthenium(II) Dichloride·$SOCl_2$·HCl (3). To a stirred suspension of bisacid **1** (0.19 g, 0.25 mmol) in CH_2Cl_2 (15 mL) was added thionyl chloride (2.5 mL), and the reaction mixture was stirred for 4 h under reflux. The solvent and the excess $SOCl_2$ were removed under reduced pressure, and the resulting dark red viscous oil was dried in vacuo at 60−70 °C for 1 h. The solid bis(acid chloride) **3** was used immediately for the macrocyclization reactions: yield 0.23 g (∼100%); ^{1}H NMR (CD_2Cl_2) δ 9.03 (br s, 2H, Pyr 3,3′), 8.77 (t, J = 7 Hz, 4H, Bp 3,3′), 8.34 (br s, 2H, Pyr 6,6′), 8.14 (t, J = 7 Hz, 4H, Bp 4,4′, and 2H, Pyr 5,5′), 7.96, 7.82 (2 br s, 2H each, Bp 6,6′), 7.57 (br s, 4H, Bp 5,5′); ^{13}C NMR (CD_2Cl_2) δ 166.6 (s, COCl), 158.0, 156.6, 156.5 (3 s, Bp and Pyr 2,2′), 154.6, 153.0, 152.0 (3 d, Pyr and Bp 6,6′), 140.6 (s, Pyr 4,4′), 139.4 (d, Bp 4,4′), 129.2, 129.0 (2 d, Bp 5,5′), 128.7 (d, Pyr 5,5′), 125.4 (br d, Bp 5,5′), 124.4 (s, Pyr 3,3′). Anal. Calcd for $C_{32}H_{23}N_6O_3SCl_7Ru$: C, 41.74; H, 2.52; N, 9.13; Cl, 26.95; Ru, 10.98. Found: C, 41.50; H, 2.95; N, 9.02; Cl, 25.03; Ru, 11.44.

4,4′-Bis[[2-[(*tert*-butoxycarbonyl)amino]ethyl]carbamoyl]-2,2′-bipyridine (4). To a stirred solution of *N*-(*tert*-butoxycarbonyl)-1,2-diaminoethane (3.3 g, 20.6 mmol) and triethylamine (2.5 g, 25 mmol) in tetrahydrofuran (40 mL) was added a solution of 4,4′-bis(chlorocarbonyl)-2,2′-bipyridine (2.9 g, 10 mmol) over 0.5 h. The reaction mixture was then stirred for 1 h under reflux and cooled to room temperature, and the white solid was separated. This was suspended in 20% ethanol (100 mL), concentrated ammonium hydroxide (2 mL) was added, and the suspension was stirred at room temperature for 1 h. After stirring, the pure bisamide **4** was separated, washed with 50% ethanol (2 × 30 mL), and dried at 60 °C: yield 4.8 g (91%); an analytical sample was recrystallized from a mixture of DMF and ethanol (1:3); mp 260−63 °C (dec); ^{1}H NMR (DMSO-d_6) δ 8.93 (t, J = 5.5 Hz, 2H, CONH), 8.88 (d, J = 5 Hz, 2H, Bp 6,6′), 8.78 (s, 2H, Pyr 3,3′), 7.83 (d, J = 5 Hz, 2H, Pyr 5,5′), 6.93 (t, J = 5.5 Hz, 2H, CONH), 3.33, 3.14 (2 q, J = 6 Hz, 4H each, NHCH_2CH_2NH), 1.35 (s, 18H, CH_3); ^{13}C NMR (DMSO-d_6) δ 164.7, 155.5 (2 s, CONH), 155.7 (s, Pyr 2,2′), 149.9 (d, Pyr 6,6′), 142.9 (s, Pyr 4,4′), 121.9 (d, Pyr 5,5′) 118.2 (d, Pyr 3,3′), 77.7 (s, *C*(CH_3)), 28.2 (q, C(*C*H_3)). Anal. Calcd for $C_{26}H_{36}N_6O_6$: C, 59.08; H, 6.86; N, 15.90. Found: C, 59.10; H, 7.09; N, 15.82.

[4,4′-Bis[[2-[(*tert*-butoxycarbonyl)amino]ethylcarbamoyl]-2,2′-bipyridine]bis(2,2′-bipyridine)ruthenium(II) Dichloride Dihydrate (5a). A mixutre of bisamide **4** (0.53 g, 1 mmol) and *cis*-Ru(bpy)$_2$Cl$_2$·2H_2O (0.52 g, 1 mmol) in 80% ethanol (70 mL) was stirred for 5 h under reflux and then concentrated in vacuo. Column chromatography

(29) Meyer, H.; Tropsch, H. *Monatsch. Chem*. **1994**, *35*, 782.
(30) Lorkowski, H. J.; Pannier, R.; Wende, A. *J. Prakt. Chem*. **1967**, *35*, 149.
(31) Sheats, J. E.; Rausch, M. D. *J. Org. Chem*. **1970**, *35*, 3245.
(32) Fabiano, E.; Golding, B. T.; Sadeghi, M. M. *Synthesis* **1987**, 190.

of the resulting dark red crude product on Sephadex LH20 eluting with acetonirtile/*i*-PrOH (93:7) afforded the dark red complex **5a**. This was obtained pure after drying in vacuo: yield 1 g (95%); ^{1}H NMR (MeCN-d_3 + 10% DMSO-d_6) δ 10.25 (d, J = 1 Hz, 2H, Pyr 3,3′), 9.31 (s, 2H CONH), 8.70 (m, 4H, Bp 3,3′), 8.07, 8.05 (2 td, J = 8 and 1 Hz, 4H, Bp 4,4′), 7.87 (dd, J = 6 and 1.5 Hz, 2H, Pyr 5,5′), 7.83 (d, J = 6 Hz, 2H, Pyr 6,6′), 7.71 (2 d, J = 5.5 Hz, 4H, Bp 6,6′), 7.42, 7.38 (2 td, J = 6 and 1 Hz, 2H each, Bp 5,5′), 6.57 (br s, 2H, OCONH), 3.43, 3.30 (2 q, J = 4.5 Hz, 4H each, NHCH_2CH_2NH), 1.33 (s, 18H, CH_3); ^{13}C NMR (MeCN-d_3 + 10% DMSO-d_6) δ 163.0 (s, CONH), 158.1, 157.2, 157.1 (3 s, Pyr and Bp 2,2′), 156.2 (s, OCONH), 152.4, 152.1, 151.8 (3 d, Pyr and Bp 6,6′), 142.0 (s, Pyr 4,4′), 138.3 (d, Bp 4,4′), 128.0, 127.9 (2 d, Bp 5,5′), 126.2 (d, Pyr 5,5′), 124.9 (d, Bp 3,3′), 122.6 (d, Pyr 3,3′), 78.4 (s, $C(CH_3)$), 40.8, 39.6 (2 t, $NHCH_2CH_2NH$), 28.1 (q, CH_3). Anal. Calcd for $C_{46}H_{56}N_{10}O_8Cl_2Ru$: C, 52.67; H, 5.38; N, 13.35; Cl, 6.76; Ru, 9.63. Found: C, 52.32; H, 5.75; N, 13.20; Cl, 6.50; Ru, 10.02.

[4,4′-Bis[[2-[(*tert*-butoxycarbonyl)amino]ethylcarbamoyl]-2,2′-bipyridine]bis(2,2′-bipyridine)osmium(II) Dichloride Dihydrate (5b). A mixture of bisamide **4** (0.27 g, 0.5 mmol) and *cis*-Os(bpy)$_2$Cl$_2$ (0.28 g, 0.5 mmol) in 80% ethanol (40 mL) was stirred for 5 h under reflux and left to stand at room temperature overnight. The dark brown solution was filtered through a celite bed, concentrated in vacuo, and dried under high vacuum at 50−60 °C to afford **5b** as a black solid which was used in the next steps without further purification: yield 0.55 g (∼100%); ^{1}H NMR (DMSO-d_6) δ 9.34 (t, J = 5.5 Hz, 2H CONH), 9.18 (s, 2H, Pyr 3,3′),8.86 (t, J = 8 Hz, 4H, Bp 3,3′), 8.04 (t, J = 8 Hz, 4H, Bp 4,4′), 7.92 (d, J = 6.5 Hz, 2H, Pyr 6,6′), 7.71 (d, J = 6.5 Hz, 2H, Pyr 5,5′), 7.67, 7.63 (2 d, J = 6 Hz, 2H each, Bp 6,6′), 7.50, 7.44 (2 t, J = 6 Hz, 2H each, Bp 5,5′), 6.55 (br s, 2H, OCONH), 3.42, 3.30 (2 q, 8H, NHCH_2CH_2NH), 1.35 (s, 18H, CH_3).

4,4′-Bis[(2-aminoethyl)carbamoyl]-2,2′-bipyridine]bis(2,2′-bipyridine)ruthenium(II) Chloride Tris(trifluoroacetate) (6a). To a solution of bisamide **5a** (0.26 g, 0.25 mmol) in CH_2Cl_2 (10 mL) was added trifluoracetic acid (25 mL), and the mixture was stirred for 2 h and then concentrated in vacuo. The residues of TFA were removed at high vacuum at 70−80 °C (1 h): yield of the dark red solid **6a** 0.27 g (100%); ^{1}H NMR (MeCN-d_3) δ 9.22 (d, J = 1.5 Hz, 2H, Pyr 3,3′), 9.18 (t, J = 5 Hz, 2H CONH), 8.51, 8.50 (ov dd, J = 8 Hz, 4H, Bp 3,3′), 8.07, 8.05 (ov td, J = 8 and 1.5 Hz, 4H, Bp 4,4′), 7.86 (br s, 6H, NH_3^+), 7.84 (d, J = 6 Hz, 2H, Pyr 6,6′), 7.74 (dd, J = 6 and 1.5 Hz, 2H, Pyr 5,5′), 7.71, 7.67 (2 dd, J = 5.5 and 1 Hz, 4H, Bp 6,6′), 7.41, 7.36 (2 td, J = 6 and 1.5 Hz, 4H, Bp 5,5′), 3.70 (m, 4H, $CH_2NH_3^+$), 3.26 (q, J = 5 Hz, 4H, CONHCH_2); ^{13}C NMR (MeCN-d_3) δ 164.9 (s, CONH), 160.6, 160.2 (2 s, CF_3*C*OOH and CF_3*C*OO$^-$), 157.7, 157.3, 157.2 (3 s, Pyr and Bp 2,2′), 152.9, 152.1 (2 d, Pyr and Bp 6,6′), 142.9 (s, Pyr 4,4′), 138.5 (d, Bp 4,4′), 128.1, 128.0 (2 d, Bp 5,5′), 126.0 (d, Pyr 5,5′), 124.8 (d, Bp 3,3′, and s, CF_3), 122.7 (d, Pyr 3,3′), 39.9, 38.0 (2 t, $NHCH_2CH_2NH_3^+$); MS-ES *m*/*z* 1083 [M − 2CF_3COOH − Cl]$^+$, 969 [M − 3CF_3COOH − Cl]$^+$, 891 [M − 4CF_3COOH]$^+$, 742 [MH − 5CF_3COOH − Cl]$^+$. Anal. Calcd for $C_{36}H_{38}N_{10}O_2Cl_2Ru$·3$CF_3COO^-$·2$CF_3$COOH: C, 41.04; H, 2.99; N, 10.40; Cl, 2.63; Ru, 7.51. Found: C, 40.01; H, 3.16; N, 9.92; Cl, 2.34; Ru, 7.52.

4,4′-Bis[(2-aminoethyl)carbamoyl]-2,2′-bipyridine]bis(2,2′-bipyridine)osmium(II) Chloride Tris(trifluoroacetate) (6b). The deprotection of **5b** (0.28 g, 0.25 mmol) was performed by the same procedure as the Ru analog **5a**: yield 0.29 g (100%). This intermediate was characterized in the next step.

Preparation of the Macrocyclic Tetraamides. General Procedures. (A) A solution of bisamide **6a** or **6b** (0.25 mmol) in acetonitrile (50 mL) and a solution of the appropriate bis(acid chloride) (0.25 mmol) in acetonitrile (50 mL), unless otherwise stated, were simultaneously added via a syringe pump to vigorously stirred acetonitrile (750 mL) containing triethylamine (0.25 g, 2.5 mmol if not stated otherwise) over 3.5 h at 45−50 °C. The mixture was stirred for 0.5 h and then concentrated in vacuo. The solid residue was extracted with methanol (50 mL) in the presence of concentrated hydrochloric acid (0.2 mL), the solid was separated and washed with methanol (2 × 20 mL), and the filtrate was concentrated in vacuo. Column chromatography of the resulting crude product on silica gel using methanol afforded the corresponding macrocycle as its chloride salt. This was converted to the PF_6 salt by addition of a large excess of NH_4PF_6 (1 g) in water (3 mL) to a vigorously stirred solution of macrocycle in water (25 mL) which produced the PF_6 salt as an orange precipitate. After 0.5 h of stirring this was separated, washed with cold water (2 × 3 mL), and dried in vacuo over P_2O_5.

(B) The solutions of bis(acid chloride) (0.25 mmol) and the corresponding diamine (0.25 mmol) in acetonitrile (50 mL each) were simultaneously added via a syringe pump to vigorously stirred acetonitrile (750 mL) containing triethylamine (0.7 mL, 5 mmol) over 3.5 h at 65−70 °C. The isolation of the products was performed by the same procedure as described above.

Macrocycle 7 was prepared according to procedure A starting from diamine **6a** (0.27 g, 0.25 mmol) and 3,5-bis(chlorocarbonyl)pyridine (0.051 g, 0.25 mmol). The eluent used was methanol containing 0.6% acetic acid. The first broad orange band is the expected 1:1 condensate: yield 0.096 g (32%); ^{1}H NMR (MeCN-d_6) δ 9.05 (s, 2H, pyr 3,3′), 9.04 (s, 2H, Dinic-Hα), 8.80 (br s, 1H, Dinic-Hγ), 8.49 (ov d, J = 8 Hz, 4H, Bp 3,3′), 8.09−8.02 (m, 4H, Bp 4,4′), 7.89 (s, 2H, CONH), 7.88 (d, J = 6 Hz, 2H, Pyr 6,6′), 7.71 (dd, J = 5 and 0.5 Hz, 2H, Pyr 5,5′), 7.70−7.67 (m, 4H, Bp 6,6′), 7.42−7.32 (m, 4H, Bp 5,5′), 3.74−3.60 (m, 8H, NHCH_2CH_2NH); ^{13}C NMR (MeCN-d_3) δ 166.4, 164.8 (2 s, CONH), 157.9, 157.2, 157.1 (3 s, Pyr and Bp 2,2′), 153.0, 152.2, 152.0 (3 d, Pyr and Bp 6,6′), 150.9 (d, Dinic-Cα), 130.0 (s, Dinic-Cβ), 128.1, 128.0 (2 d, Bp 5,5′), 125.2 (d, Pyr 5,5′), 124.8 (d, Bp 3,3′), 122.6 (d, Pyr 3,3′), 41.5, 41.3 (2 t, NH*C*H$_2$CH_2NH); MS-ES *m*/*z* 908 [M − 2PF_6]$^+$, 873 [M − 2PF_6 − 2H_2O]$^+$. Anal. Calcd for $C_{43}H_{41}N_{11}O_6P_2F_{12}Ru$: C, 43.08; H, 3.45; N, 12.85; Ru, 8.43. Found: C, 43.05; H, 3.58; N, 12.52; Ru, 8.61.

Macrocycle 8 was prepared according to procedure A starting from diamine **6a** (0.27 g, 0.25 mmol) and 1,1′-bis(chlorocarbonyl)ferrocene (0.078 g, 0.25 mmol). The eluent used was methanol containing 0.4% acetic acid. The PF_6 salt was separated immediately after the precipitation: yield 0.11 g (36%); ^{1}H NMR (MeCN-d_6) δ 9.05 (s, 2H, Pyr 3,3′), 8.49 (ov dd, J = 7 Hz, 4H, Bp 3,3′), 8.28 (br s, CONH), 8.07, 8.04 (2 t, J = 8 Hz, 2H each, Bp 4,4′), 7.85 (d, J = 5.5 Hz, 2H, Pyr 6,6′), 7.71 (ov d, J = 7 Hz, 4H, Bp 6,6′), 7.64 (d, J = 5.5 Hz, 2H, Pyr 5,5′), 7.48, 7.35 (2 t, J = 7 Hz, 2H each, Bp 5,5′), 7.24 (br s, CONH), 4.67 (d, J = 13.5 Hz, 4H, Fc-Hα), 4.36 (d, J = 17.5 Hz, 4H Fc-Hβ), 3.67−3.54 (m, 8H, NHCH_2CH_2NH); ^{13}C NMR (MeCN-d_3) δ 171.4, 164.5 (2 s, CONH), 157.8, 157.3, 157.2 (3 s, Pyr and Bp 2,2′), 153.1, 152.1, 152.0 (3 d, Pyr and Bp 6,6′), 143.1 (s, Pyr 4,4′), 138.5 (d, Bp 4,4′), 128.1, 128.0 (2 d, Bp 5,5′), 125.7 (d, Pyr 5,5′), 124.8 (d, Bp 3,3′), 122.3 (d, Pyr 3,3′), 78.0 (s, Fc-C_{ipso}), 73.0, 70.0 (2 d, Fc-Cα and Cβ), 41.7, 40.3 (2 t, NH*C*H$_2$CH_2NH); MS-FAB *m*/*z* 1125 [MH − PF_6 − 2H_2O]$^+$, 979 [MH − 2PF_6 − 2H_2O]$^+$. Anal. Calcd for $C_{48}H_{46}N_{10}O_6P_2F_{12}RuFe$: C, 44.15; H, 3.55; N, 10.73; Ru, 7.74. Found: C, 43.81; H, 3.46; N, 10.54; Ru, 7.80.

Macrocycle 9 was prepared according to procedure A starting from diamine **6a** (0.27 g, 0.25 mmol) and 1,1′-bis(chlorocarbonyl)cobaltocenium (0.11 g, 0.25 mmol). The eluent used was methanol containing 1.2% acetic acid. The third (dark orange) band is the expected macrocycle: yield 0.05 g (13%); ^{1}H NMR (MeCN-d_6) δ 8.99 (br s, 2H, Pyr 3,3′), 8.52 (m, 4H, Bp 3,3′) 8.11−8.05 (m, 4H, Bp 4,4′ and 2H CONH), 7.83 (d, J = 6 Hz, 2H, Pyr 6,6′), 7.73−7.69 (m, 4H, Bp 6,6′, 2H, Pyr 5,5′, and 2H, CONH), 7.42, 7.39, (2 td, J = 5.5 and 1.5 Hz, 2H each, Bp 5,5′), 6.31 (dt, J = 37 and 1.5 Hz, 4H, Co-Hα), 5.78 (dm, J = 20 and 1.5 Hz, 4H, Co-Hβ), 3.73−3.45 (m, 8H, NHCH_2CH_2-NH); ^{13}C NMR (MeCN-d_3) δ 163.5, 161.8 (2 s, CONH), 158.1, 157.3, 157.2 (3 s, Pyr and Bp 2,2′), 152.6, 152.3, 152.0 (3 d, Pyr and Bp 6,6′), 142.6 (s, Pyr 4,4′), 138.4 (d, Bp 4,4′), 128.2, 128.0 (2 d, Bp 5,5′), 126.3 (d, Pyr 5,5′), 124.9 (d, Bp 3,3′), 123.0 (d, Pyr 3,3′), 95.0 (s, Co-C_{ipso}), 88.5, 88.3 (2 d, Co-Cα), 85.9, 85.7 (2 d, Co-Cβ), 40.6, 40.5 (2 t, NHCH_2CH_2NH); MS-FAB *m*/*z* 1273 [MH − PF_6 − 2$H_2$0]$^+$, 1128 [MH −2PF_6 − 2$H_2$0]$^+$. Anal. Calcd for $C_{48}H_{48}N_{10}O_7P_3F_{18}$-CoRu: C, 39.66; H, 3.28; N, 9.53; Ru, 6.87. Found: C, 38.85; H, 3.47; N, 9.73; Ru, 6.87.

Macrocycle 10 was prepared according to procedure A starting from diamine **6a** (0.27 g, 0.25 mmol) and 4,4′-bis(chlorocarbonyl)2,2′-bipyridine (0.07 g, 0.25 mmol). The eluent used was methanol containing 0.8% acetic acid. The PF_6 salt was prepared using KPF_6: yield 0.08 g (25%); ^{1}H NMR (MeCN-d_6) δ 8.80 (br s, 2H, CONH), 8.75 (d, J = 5 Hz, 2H, Pyr 6,6′), 8.61 (br s, 2H, Pyr(Ru) 3,3′), 8.46

(m, 4H, Bp 3,3′), 8.05, 8.01 (2 t, $J = 8$ Hz, 2H each, Bp 4,4′), 7.82 (d, $J = 6$ Hz, 2H, Pyr 6,6′, and 2H, CONH), 7.76 (d, $J = 5$ Hz, 2H, Pyr 5,5′), 7.65, 7.56 (2 d, $J = 6$ Hz, 2H each, Bp 6,6′), 7.58 (dd, $J = 6$ and 1.5 Hz, 2H, Pyr(Ru) 5,5′), 7.38, 7.28 (2 t, $J = 6.5$ Hz, 2H each, Bp 5,5′), 3.78−3.63 (m, 8H, NHCH_2CH_2NH); ^{13}C NMR (MeCN-d_3) δ 165.8, 164.5 (2 s, CONH), 157.9, 157.2, 157.1 (3 s, Pyr(Ru) and Bp 2,2′), 154.4 (s, Pyr 2,2′), 152.9, 152.0, 151.9 (3 d, Pyr (Ru) and Bp 6,6′), 150.0 (d, Pyr 6,6′), 144.8, 142.7 (2 s, Pyr and Pyr(Ru) 4,4′), 138.5 (d, Bp 4,4′), 128.1, 128.0 (2 d, Bp 5,5′), 124.8 (d, Pyr(Ru) 5,5′ and Bp 3,3′), 122.6 (d, Pyr 3,3′), 122.5 (d, Pyr 5,5′), 120.7 (d, Pyr (Ru) 3,3′), 40.9, 40.7 (2 t, NHCH_2CH_2NH); MS-FAB *m*/*z* 1066/7 [MH − 2PF_6]$^+$, 1095 [MH − PF_6 − H_2O]$^+$. Anal. Calcd for $C_{48}H_{48}N_{12}O_8P_2F_{12}Ru$: C, 43.94; H, 3.69; N, 12.81; Ru, 7.70. Found: C, 43.50; H, 3.63; N, 12.40; Ru, 7.57.

Macrocycle 11 was prepared according to procedure A starting from diamine **6a** (0.27 g, 0.25 mmol) and bis(acid chloride) **3** prepared from bisacid **2** (0.19 g, 0.25 mmol) in the presence of triethylamine (0.3 g, 0.3 mmol). The eluent used was methanol containing 0.8% acetic acid: yield 0.17 g (32.7%); ^{1}H NMR (MeCN-d_3) δ 9.11 (br s, 4H, Pyr 3,3′), 8.52−8.48 (m, 8H, Bp 3,3′), 8.10−8.05 (m, 8H, Bp 4,4′), 7.91 (br s, 4H CONH), 7.86 (m, 4H, Pyr 6,6′), 7.73−7.63 (m, 8H, Bp 6,6′ and 4H Pyr 5,5′), 7.44−7.30 (m, 8H, Bp 5,5′), 3.73 (br t, 8H, NHCH_2CH_2NH); ^{13}C NMR (MeCN-d_3) δ 164.5 (br s, CONH), 157.9, 157.3, 157.1 (3 s, Pyr and Bp 2,2′), 152.9, 152.0 (3 d, Pyr and Bp 6,6′), 142.8 (br s, Pyr 4,4′), 138.6 (d, Bp 4,4′), 128.2, 128.0 (2 d, Bp 5,5′), 125.2 (br d, Pyr 5,5′), 124.8 (d, Bp 3,3′), 122.5 (br d, Pyr 3,3′), 40.9 (br t, NHCH_2CH_2NH). Anal. Calcd for $C_{68}H_{64}N_{16}O_8P_4F_{24}Ru_2$: C, 40.53; H, 3.20; N, 11.12. Found: C, 40.32; H, 3.16; N, 11.10.

Macrocycle 12 was prepared according to procedure A starting from bis(acid chloride) **3** prepared from bisacid **2** (0.19 g, 0.25 mmol) and diamine **6b** (0.29 g, 0.25 mmol) in the presence of triethylamine (0.3 g, 0.3 mmol). The eluent used was methanol containing 0.8% acetic acid: yield of the dark green powder **12** 0.21 g (40%); ^{1}H NMR (MeCN-d_3) δ 9.07 (br s, 4H, Pyr 3,3′), 8.49−8.45 (m, 8H, Bp 3,3′-(Ru)), 8.09−8.04 (m, 4H, Bp 4,4′ (Ru)), 7.92−7.87 (m, 4H, Bp 4,4′ (Os), and 2H, CONH), 7.85, 7.78 (2 d, $J = 6$ and 1.5 Hz, 2H each, Pyr 6,6′(Os, Ru)), 7.68, 7.58 (2 m, 2H each, Bp 6,6′), 7.63 (m, 2H, Bp 6,6′, and 2H, Bp 5,5′), 7.51 (m, 2H, Bp 6,6′, 2H Pyr 5,5′, and 2H, CONH), 7.42−7.21 (m, 8H, Bp 5,5′(Os,Ru)), 3.81−3.59 (m, NHCH_2CH_2-NH); ^{13}C NMR (MeCN-d_3) δ 164.7 (br s, CONH), 160.2, 159.1 157.9, 157.2, 157.1 (6 s, Pyr and Bp 2,2′), 152.9, 152.1, 152.0, 152.0, 151.3, 151.1 (6 d, Pyr and Bp 6,6′), 142.8, 141.8 (2 s, Pyr 4,4′), 138.6, 138.1 (2 d, Bp 4,4′), 128.6, 128.5, 128.2, 128.0 (4 d, Bp 5,5′), 125.8, 125.0 (2 d, Pyr 5,5′), 125.0, 124.8 (2 d, Bp 3,3′), 122.7 (d, Pyr 3,3′), 122.5 (d, Pyr 3,3′), 41.0 (t, NHCH_2CH_2NH); MS-ES *m*/*z* 872 [MH − 2PF_6 − 2H_2O]$^{2+}$, 817 [MH − 3PF_6 − 2H_2O]$^{2+}$. Anal. Calcd for $C_{68}H_{64}N_{16}O_8P_4F_{24}RuOs$: C, 38.81; H, 3.07; N, 10.65; Ru, 4.80. Found: C, 39.30; H, 3.20; N, 10.65; Ru, 4.89.

Macrocycle 13 was prepared according to procedure B starting from bis(acid chloride) **3** prepared from bisacid **2** (0.19 g, 0.25 mmol) and *m*-phenylenediamine (0.027 g, 0.25 mmol). The eluent used was methanol containing 1.5% acetic acid. The last moving dark orange band was the 2:2 condensate: yield 0.12 g (46%) of red powder; ^{1}H NMR (DMSO-d_6) δ 11.14 (br s, 4H, CONH), 9.63 (br s, 4H, Pyr 3,3′), 8.93 (ov d, 8H, Bp 3,3′), 8.73 (br s, 2H, Ph-H2), 8.29−8.23 (m, 8H, Bp 4,4′), 8.11 (d, $J = 5.5$ Hz, 4H, Pyr 5,5′), 8.05 (d, $J = 5.5$ Hz, 4H, Pyr 6,6′), 7.84−7.80 (m, 8H, Bp 6,6′, and 4H, Ph-H4,6), 7.62, 7.56 (2 t, $J = 6$ Hz, 4H each, Bp 5,5′), 7.47 (t, $J = 8$ Hz, 2H, Ph-H5); ^{13}C NMR (DMSO-d_6) δ 161.9 (s, CONH), 157.1, 156.6, 156.4 (3 s, Pyr and Bp 2,2′), 152.2, 151.5, 151.3 (3 d, Pyr and Bp 6,6′), 141.9 (s, Pyr 4,4′), 138.8 (s, PhC1,3), 138.3 (d, Bp 4,4′), 129.4 (d, PhC5), 128.0, 127.9 (2 d, Bp 5,5′), 125.7 (d, Pyr 5,5′), 124.6 (d, Bp 3,3′), 122.9 (d, Pyr 3,3′), 116.6 (d, PhC4,6), 113.1 (d, PhC2); MS-ES *m*/*z* 1749 [MH − 2PF_6 − 4H_2O]$^+$, 1604 [MH − 3PF_6 − 4H_2O]$^+$, 802 [MH − 3PF_6 − 4H_2O]$^{2+}$. Anal. Calcd for $C_{76}H_{64}N_{16}O_8P_4F_{24}Ru_2$: C, 43.23; H, 3.06; N, 10.61; Ru, 9.57. Found: C, 42.90; H, 3.06; N, 10.34; Ru, 9.87.

Macrocycle 14 was prepared according to procedure B starting from bis(acid chloride) **3** prepared from bisacid **2** (0.19 g, 0.25 mmol) and 1,4-diamino-2-butyne (0.021 g, 0.25 mmol). The eluent used was methanol containing 0.8% acetic acid: yield 0.09 g (31%) of red powder; ^{1}H NMR (MeCN-d_3) δ 8.95 (br s, 4H, Pyr 3,3′), 8.53, 8.52 (ov d, 8H, Bp 3,3′), 8.12−8.06, (m, 8H, Bp 4,4′), 7.92 (d, $J = 6$ Hz, 4H, Pyr 6,6′), 7.87 (br s, 4H, CONH), 7.73−7.70 (m, 8H, Bp 6,6′, and 4H, Pyr 5,5′), 7.44, 7.39 (2 t, $J = 6$ Hz, 4H each, Bp 5,5′), 4.22 (d, $J = 5$ Hz, 8H, $NHCH_2$); ^{13}C NMR (DMSO-d_6) δ 163.3 (s, CONH), 158.0, 157.2, 157.1 (3 s, Pyr and Bp 2,2′), 153.1, 152.5, 152.0 (3 d, Pyr and Bp 6,6′), 142.1 (s, Pyr 4,4′), 138.6 (d, Bp 4,4′), 128.2, 128.1 (2 d, Bp 5,5′), 125.4 (d, Pyr 5,5′), 124.8 (d, Bp 3,3′), 122.4 (d, Pyr 3,3′), 78.7 (2 s, C≡C), 29.7 (t, $NHCH_2$); MS-ES *m*/*z* 1846 [MH − PF_6 − 4H_2O]$^+$, 1702 [MH − 2PF_6 − 4H_2O]$^+$. Anal. Calcd for $C_{72}H_{64}N_{16}O_8P_4F_{24}Ru_2$: C, 41.91; H, 3.13; N, 10.86; Ru, 9.80. Found: C, 41.63; H, 2.87; N, 10.59; Ru, 9.67.

Macrocycle 15 was prepared according to procedure B starting from bis(acid chloride) **3** prepared from bisacid **2** (0.19 g, 0.25 mmol) and 1,3-diaminopropane (0.0185 g, 0.25 mmol). The eluent used was methanol containing 0.8% acetic acid: yield 0.045 g (17.5%); ^{1}H NMR (MeCN-d_3) δ 9.15, 9.14 (2 ov d, $J = 1$ Hz,4H, Pyr 3,3′), 8.52, (dd, $J = 7.5$ and 1 Hz, 8H, Bp 3,3′), 8.10−8.05 (m, 8H, Bp 4,4′), 7.93 (d, $J = 6$ Hz, 4H, Pyr 6,6′), 7.79 (br s, 4H, CONH), 7.74−7.69 (m, 8H, Bp 6,6′, and 4H, Pyr 5,5′), 7.44−7.37 (m, 8H, Bp 5,5′), 3.56 (q, $J = 6$ Hz, 8H, NHCH_2CH_2CH_2NH), 1.87 (br s, NHCH_2CH_2CH_2NH); ^{13}C NMR (MeCN-d_3) δ 164.5 (s, CONH), 158.0, 157.3, 157.1 (3 s, Pyr and Bp 2,2′), 153.1, 152.2, 152.1 (3 d, Pyr and Bp 6,6′), 143.4 (s, Pyr 4,4′), 138.6 (d, Bp 4,4′), 128.2, 128.1 (2 d, Bp 5,5′), 125.5 (d, Pyr 5,5′), 124.8 (d, Bp 3,3′), 122.2 (d, Pyr 3,3′), 35.6 (t, NHCH_2CH_2CH_2NH), 28.0 (t, NHCH_2CH_2CH_2NH). Anal. Calcd for $C_{70}H_{68}N_{16}O_8P_4F_{24}Ru_2$: C, 41.15; H, 3.35; N, 10.97; Ru, 9.89. Found: C, 40.96; H, 3.50; N, 10.86; Ru, 9.89.

Macrocycle 16 was prepared according to procedure B starting from bis(acid chloride) **3** prepared from bisacid **2** (0.19 g, 0.25 mmol) and 1,4-diamino-2-butane (0.022 g, 0.25 mmol). The eluent used was methanol containing 0.8% acetic acid: yield 0.06 g (23%); ^{1}H NMR (MeCN-d_3) δ 8.90 (br s, 4H, Pyr 3,3′), 8.49 (ov d, 8H, Bp 3,3′), 8.09−8.03 (m, 8H, Bp 4,4′), 7.86(d, $J = 6$ Hz, 4H, Pyr 6,6′), 7.70−7.66 (m, 8H, Bp 6,6′, and 4H, Pyr 5,5′), 7.51 (br s, CONH), 7.40, 7.35 (2 td, $J = 6$ and 1.5 Hz, 4H each, Bp 5,5′), 3.47 (br s, 8H, NHCH_2CH_2CH_2CH_2-NH), 1.71 (br s, 8H, NHCH_2CH_2CH_2CH_2NH); ^{13}C NMR (MeCN-d_3) δ 16.34 (s, CONH), 157.8, 157.2, 157.1 (3 s, Pyr and Bp 2,2′), 152.9, 152.0 (2 d, Pyr and Bp 6,6′), 143.1 (s, Pyr 4,4′), 138.5 (d, Bp 4,4′), 128.1, 128.0 (2 d, Bp 5,5′), 125.4 (d, Pyr 5,5′), 124.8 (d, Bp 3,3′), 122.3 (d, Pyr 3,3′), 40.2 (t, NHCH_2CH_2CH_2CH_2NH), 26.9 (t, NHCH_2CH_2CH_2CH_2NH). Anal. Calcd for $C_{72}H_{72}N_{16}O_8P_4F_{24}Ru_2$: C, 41.75; H, 3.50; N, 10.82; Ru, 9.76. Found: C, 41.50; H, 3.12; N, 10.36; Ru, 9.82.

Crystal Structure Determinations. Crystal data are given in Table 5, together with refinement details. Data for the three crystals were collected with Mo Kα radiation using the MARresearch Image Plate System. The crystals were positioned at 75 mm from the image plate. Ninety-five frames were measured at 2° intervals with a counting time of 2 min. Data analysis was carried out with the XDS program.[33] All three structures were solved using direct methods with the Shelx86 program.[34] In the three structures the non-hydrogen atoms in the macrocycle cations were refined with anisotropic thermal parameters. The hydrogen atoms were included in geometric positions. In all three structures, however, the anions and solvent molecules were disordered. In the bromide complex of **7** one bromide ion was disordered over two sites and there were three disordered solvent molecules, one ethanol with 0.5 occupancy, one ethanol disordered over two positions, and one methanol with 0.5 occupancy. In the chloride complex of **7** one chloride ion was disordered over five sites and there were six sites refined as solvent water each with 0.25 occupancy. In **13**·2OAc for each dimeric cation, there was one ordered acetate, one acetate with 50% occupancy, and one PF_6^- with 50% occupancy. In addition there were three water molecules with 0.33 occupancy and two ethanol molecules and one methanol molecule each with 0.50 occupancy. In the three structures, disordered ions and solvent molecules were refined isotropically with hydrogen atoms not included. All structures were refined on F^2 using Shelxl.[35] All calculations were carried out on a Silicon Graphics R4000 workstation at the University of Reading.

(33) Kabsch, W. *J. Appl. Crystallogr.* **1988**, *21*, 916.
(34) Shelx86, Sheldrick, G. M. *Acta.Crystallogr.* **1990**, *A46*, 467.
(35) Shelxl, program for crystal structure refinement: Sheldrick, G. M. University of Gottingen, 1993.

Table 5. Crystal Data and Structure Refinement for **7**·2Br$^-$, **7**·Cl$^-$ and **13**·2OAc$^-$

	7·2Br$^-$	**7**·Cl$^-$	**13**·2OAc$^-$
formula	**7**·2Br$^-$·1.5C_2H_5OH·0.5CH_3OH	**7**·2Cl$^-$·C_2H_6SO·1.5H_2O	**13**·3$CH_3CO_2^-$·PF_6^-·H_2O·C_2H_5OH·CH_3OH
empirical formula	$C_{46.5}H_{47}Br_2N_{11}O_6Ru$	$C_{45}H_{43}Cl_2N_{11}O_{6.5}SRu$	$C_{89}H_{85}F_6N_{14}O_{15}PRu_2$
formula weight	1116.7	1048.9	1937.8
temperature (K)	293(2)	293(2)	293(2)
wavelength (Å)	0.710 73	0.710 73	0.710 73
crystal system	triclinic	monoclinic	triclinic
space group	$P\bar{1}$	$P2_1/n$	$P\bar{1}$
unit cell dimensions: a (Å)	13.395(9)	20.351(17)	13.533(14)
b (Å)	13.813(12)	14.641(14)	13.582(13)
c (Å)	16.713(14)	23.503(21)	17.56(2)
α (deg)	73.235(1)	(90)	104.19(1)
β (deg)	66.610(1)	109.00(1)	94.03(1)
γ (deg)	79.166(1)	(90)	111.74(1)
volume (Å^3)	2708	6621	2860
Z	2	4	1
density (calculated) Mg/m^3	1.370	1.052	1.125
absorption coefficient mm^{-1}	1.82	0.39	0.34
F(000)	1130	2156	994
crystal size (mm)	0.35 × 0.35 × 0.25	0.30 × 0.25 × 0.25	0.35 × 0.25 × 0.20
θ range for data collection (deg)	2.61−25.03	2.30−25.10	3.04−24.97
index ranges	$0 \le h \le 15$, $-14 \le k \le 15$, $-17 \le l \le 19$	$0 \le h \le 24$, $-16 \le k \le 16$, $-27 \le l \le 26$	$-16 \le h \le 15$, $-15 \le k \le 14$, $0 \le l \le 20$
reflections collected	7685	20163	8697
independent reflections [R(int)]	7685	11038 [0.0934]	8697
weighting scheme (a, b)[a]	0.726, 0.000	0.344, 0.000	0.213, 0.000
data/restraints/parameters	7685/0/600	11038/0/624	8697/0/553
goodness-of-fit on F^2	1.091	1.049	1.023
final R indices [$I > 2\sigma(I)$]	$R_1 = 0.1043$,	0.0844	0.1219
	$wR_2 = 0.2560$	0.1676	0.3319
R indices (all data)	$R_1 = 0.1845$,	0.1915	0.2028
	$wR2 = 0.2982$	0.2018	0.3924
extinction coefficient	0.034(3)	0.0031(3)	0.0000(14)
largest diff peak and hole (e·Å^{-3})	0.990 and −1.207	0.551, −0.432	0.817, −0.557

[a] Weighting scheme $w = 1/(\sigma^2(F_o^2) + (aP)^2 + (bP)$, where $P = (F_o^2 + 2F_c^2)/3$.

Acknowledgment. We thank the EPSRC for a postdoctoral fellowship (F.S.) and Kodak Limited for a studentship (S.W.D.). We also thank the EPSRC for use of the mass spectrometry service at University College Swansea and the University of Reading for funds for the image plate system. Johnson Matthey is acknowledged for the generous loan of ruthenium trichloride.

Supporting Information Available: Tables of positional parameters, bond lengths, bond angles, anisotropic thermal parameters, and hydrogen positions for **7**·2Br$^-$, **7**·Cl$^-$, and **13**·2OAc$^-$ (31 pages). See any current masthead page for ordering and Internet access instructions.

JA9725099